



## Effect of Electrical Coupling at The Border on The 1D Biological Pacemaker – A Simulation Study\*

ZHANG Yue<sup>1,2)</sup>, LIU Shu-Yong<sup>1)\*\*</sup>, LI Jie<sup>3)</sup>, WANG Kuan-Quan<sup>4)</sup>

<sup>1)</sup>College of Computer Science and Technology, Harbin Engineering University, Harbin 150001, China;

<sup>2)</sup>School of Computer Science and Engineering, University of New South Wales, Sydney, NSW 2052, Australia;

<sup>3)</sup>School of Electrical Engineering, Yanshan University, Qinhuangdao 066004, China;

<sup>4)</sup>School of Computer Science and Technology, Harbin Institute of Technology, Harbin 150001, China)

**Abstract** Biological pacemaker has attracted more and more attention of the researchers. The aim of this manuscript is to investigate the effect of the electrical coupling at the border on the pacing and driving of the biological pacemaker in ventricle. First of all, a 1D ventricular strand model containing a pacemaker is developed by using the anisotropic reaction diffusion equation. Based on the model, the initial pacing time(IPT), action potentials of the cells in special locations, and the propagation process of the electrical excitation are simulated corresponding to different couplings at the border, and it is found that to an extent, the pacing of the pacemaker is enhanced by weakening the coupling. However, when the coupling is small enough, the excitation of the pacemaker could not effuse, making the driving failed. In addition, the relationship between the minimum size of the pacemaker and the coupling is also probed, which reveals that the smaller the coupling is, the less the pacing cells are required. Nevertheless, the relationship is not prominent. In conclusion, it plays a certain role in the functioning of the pacemaker to reduce the coupling at the border alone. Nevertheless, other measures should also be taken to create an effective biological pacemaker.

**Key words** biological pacemaker, ventricular myocytes, pacing, driving, electrical coupling

**DOI:** 10.16476/j.pibb.2019.0327

Heart is one of the indispensable organs in the human body. However, cardiovascular diseases have been the first killer of the human health in recent years, resulting in more than 3.5 million deaths every year in China alone<sup>[1]</sup>, in which, sinus node dysfunction and atrioventricular block are the most common types. The best way to treat these diseases is to implant electrical devices, which have been employed for more than 6 decades with refinements. In the United States, there are more than 200 000 patients who need to implant electrical pacemakers every year<sup>[2]</sup>. Meanwhile, the disadvantages of the devices are transparent, such as the infection, short battery lifespan and so on<sup>[3-6]</sup>. As a result, more and more attention has been paid to the biological pacemakers<sup>[7-10]</sup>.

In the normal heart, there are no more than  $10^4$  pace-making cells, which produce electrical impulses automatically and drive the whole heart containing about  $10^{10}$  cells<sup>[11]</sup>. The ratio of the pace-making cells

and all the cardiac cells is about  $1 : 10^6$ . In a previous study of the biological pacemaker, a 2D computing model was developed and it was found that the pacemaker could not work even though the ratio was  $1 : 3$ , if the coupling in the ventricle tissue and biological pacemaker was with normal value<sup>[12]</sup>. So, what contributes most to the robust functioning of an efficient pacemaker?

In fact, a salient feature of the genuine pacemaker — the sinoatrial node (SAN) is that the electrical coupling in SAN is weaker than that in the

---

\* This work was supported by grants from The National Natural Science Foundation of China (61701135), The China Postdoctoral Science Foundation(2018M630342), The Natural Science Foundation of Heilongjiang Province (QC2018075), and The Natural Science Foundation of Hebei Province (F2019203569).

\*\* Corresponding author.

Tel: 13091439889, E-mail: liushuyong@hrbeu.edu.cn

Received: December 22, 2019 Accepted: April 3, 2020

atrial and ventricular tissues. Moreover, the coupling is much weaker in the core and is a little stronger at the periphery<sup>[13-14]</sup>.

SAN is given rise to by the Tbx18-expressing mesenchymal precursor cells<sup>[15-16]</sup>. The overexpression of Tbx18 significantly down-regulates Cx43 in the center, while does not make negative impact on Cx40 and Cx45 at the periphery of SAN. On one hand, the depression of Cx43 leads to the substantial decline of electrical coupling in the SAN. On the other hand, the sufficient connexins Cx40 and Cx45 at the periphery guarantee the electrical connection between SAN and the cardiac tissue<sup>[17-20]</sup>.

The weak coupling in the core shields the SAN from the depression of the low potential environment of the adjacent cardiac tissue, contributing to the depolarization of the pacemaker. And, the stronger coupling at the periphery provides the sufficient electrical connection between the SAN and the cardiac tissue, making sure that the high potential from the depolarizing pacemaker stimulates the neighboring cardiac cells to depolarize, leading to the electrical excitation spread in the heart<sup>[21-23]</sup>. That is, the weak coupling plays an important role in the functioning of SAN, and it might also be an efficient method to weaken the coupling to generate an effective biological pacemaker in the ventricle.

In view of the development of SAN, Tbx18 was injected directly into the ventricle in order to create biological pacemakers<sup>[24-26]</sup>. The experimental results indicated that the coupling in the injection area was weakened and the ventricular myocytes were capable of pacing.

From the research of SAN and the biological pacemakers, the weak coupling is the common factor for the successful pacing and driving.

In a previous study, the effect of weakening the electrical coupling inside the pacemaker was investigated in a 2D slice, and it is found that the number of the pacing cells required decreased with the coupling weakened<sup>[27]</sup>. A 4-fold decrease of coupling led to a 4-fold reduction of the pacing cells. In the research of Weiss *et al.*<sup>[28]</sup>, a 6.25-fold decrease of coupling in the pacemaker reduced the pacing cells required by about 2.5 fold in 1D tissue, which validated the effect of the weak coupling on the pacing.

Many studies have been done on the weak coupling in the whole pacemaker. How about the

effect of the weak coupling at the border alone? Will the functioning of the pacemaker be enhanced substantially with the decline of the coupling at the border?

In the study, a 1D strand model consisting of the pacemaker and the ventricular tissue is developed. And then, the effect of the electrical coupling at the border is probed from the following 3 aspects: the initial pacing time (IPT), the action potential (AP) of cells in special locations, and the minimum size of pacemaker for successful pacing and driving.

## 1 Models and methods

The models of the single cell and 1D tissue are introduced in this section.

### 1.1 Model of the single cell

The model of the single pacing cell is based on the well-established TNNP 2006 model of human ventricular cells<sup>[29]</sup>, the detail of which is given in equations (1) and (2).

$$\frac{dV}{dt} = -\frac{I_{ion} + I_{stim}}{C_m} \quad (1)$$

$$I_{ion} = I_{Na} + I_{K1} + I_{to} + I_{Kr} + I_{Ks} + I_{CaL} + I_{NaK} + I_{NaCa} + I_{pK} + I_{pCa} + I_{bCa} + I_{bNa} \quad (2)$$

where,  $V$  is the action potential;  $t$  is the time;  $I_{ion}$  is the sum of the transmembrane ion channels; there are 12 currents including potassium channels, sodium channels and so on;  $I_{stim}$  is the external stimulus current which is set to 0 in the study;  $C_m$  is the membrane capacitance. In our simulation, for the endocardial cells, the original model is used directly; and for the pacing cells,  $G_{K1}$ , the maximum conductance of  $I_{K1}$ , is set to 0.05 nS/pF to guarantee the successful pacing.

### 1.2 1D tissue model

In the simulation, the 1D strand, 60 mm long and consisting of 401 cells, is divided into three segments (Figure 1). In the central region, it is the pacemaker with variable size, and the light gray parts of the strand are the ventricular tissue, which are made up of endocardial myocytes.

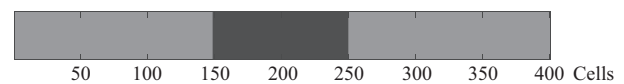


**Fig. 1 The strand**

The central area: the pacemaker; the other regions: the ventricular tissue.

The reaction - diffusion equation is adopted to describe the conduction of the electrical excitation in the strand, which is shown in equation (3):

$$\frac{\partial V}{\partial t} = -\frac{I_{ion} + I_{stim}}{C_m} + D\Delta V \quad (3)$$

where,  $D$ , the diffusion coefficient, represents the electrical coupling among the cells.  $\Delta$  is the Laplace operator. The other parameters are the same as those in equations (1) and (2).

On the 1D level, equation (3) could be discretized as the partial differential equation:

$$\begin{aligned} \frac{\partial V_i}{\partial t} = & -\frac{I_{ion} + I_{stim}}{C_m} + D_{i-1}(V_{i-1} - V_i) \\ & + D_i(V_{i+1} - V_i) \end{aligned} \quad (4)$$

where,  $V_i$  is the potential of the  $i^{\text{th}}$  cell in Figure 1;  $D_i$  is the coupling between the  $i^{\text{th}}$  and the  $(i+1)^{\text{th}}$  cells.

The coupling at the border of the pacemaker and ventricular tissue is modulated by a variable  $D$ ; and in the other region,  $D$  is set to the normal value  $0.154 \text{ cm}^2/\text{s}$ [29]. In the strand, the electrophysiological characteristics of the same type of cells are supposed to be the same. The model is solved with the time step  $0.02 \text{ ms}$  and the space step  $0.15 \text{ mm}$ . All the simulation time is not less than  $150\,000 \text{ ms}$  to gain a stable state.

## 2 Results and discussion

In this section, the simulation results are presented and discussed.

Firstly, the basic AP shape of the single pacing cell is displayed, compared with that of the single ventricular myocyte. Afterwards, the effect of the coupling is investigated in four aspects: IPT, APs of cells in special locations of the strand, the impulses spatiotemporal propagation, and the minimum number of the pacing cells required.

### 2.1 APs of the single cell

The biological pacemaker is composed of pacing cells which are reformed from the ventricular myocytes by depressing  $I_{K1}$ . What's more, the less the  $I_{K1}$ , the stronger the pacing. However, in practical experiments, it is arduous to depress  $I_{K1}$  completely. As a consequence,  $G_{K1}$  is set to  $0.05 \text{ nS/F}$ ,  $0.9\%$  of the normal value. Then, the ventricular myocytes are transformed into pacing cells and able to pace automatically and robustly without external stimulus. When the pacing reaches a stable state, a whole AP is intercepted, together with a AP of the normal

ventricular myocyte(Figure 2).

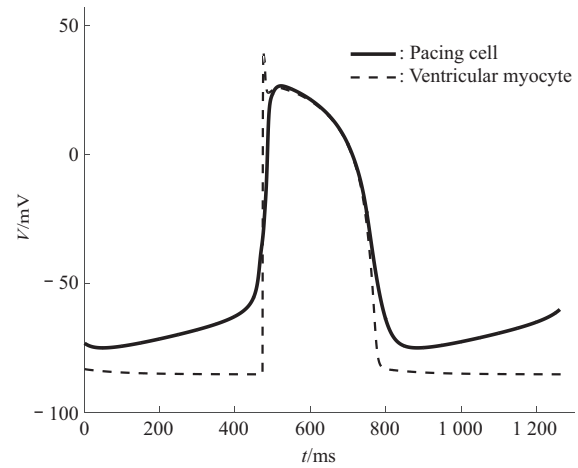


**Fig. 2 The curves of action potential ( AP )**

The solid curve describes the AP of pacing cell, and the dash line is the AP of the ventricular myocyte.

In Figure 2, the solid line represents a whole AP of the pacing cell, while the dashed one describes the AP of the endocardial myocyte. For the pacing cell, the AP emerges automatically. However, for the ventricular myocyte, the whole AP is inspired by an external  $-52 \text{ pA/pF}$  stimulus for  $1 \text{ ms}$  at  $470 \text{ ms}$ .

For the single cell, it is not difficult to discover that the lowest potential ( $-75.1 \text{ mV}$ ) of the pacing cell is palpably higher than that ( $-85.3 \text{ mV}$ ) of the ventricular myocyte. It is in that for pacing cell the dropping of the AP in the end of the 3<sup>rd</sup> phase is weakened by the depression of  $I_{K1}$ , leading to a higher AP in the 4<sup>th</sup> phase, which is favorable to the next depolarization. That is, it is more beneficial to generate an automatic depolarization.

On the 1D level, the AP of pacemaker is influenced by the surrounding ventricular myocytes as well. The bridge is the electrical coupling at the border, whose effect on the pacing and driving of the pacemaker is discussed in the following.

### 2.2 The initial pacing time

In this section, the 131 cells at the center of the strand in Figure 1 are set as the pacemaker, and the others are the endocardial myocytes.

The initial pacing time (IPT) is defined as the time when the potential of the ventricular cell adjacent to the pacemaker reaches the peak value for the first time in its successful depolarization by the driving of

the excitation from the biological pacemaker.

The capacity of the pacemaker could be described by IPT to an extent. A longer IPT might infer a weaker pacemaker.

The electrical coupling at the border is modulated by a fractional term  $x$ , where  $0 < x < 1$  represents the degree of the down-regulation of the coupling. And the coupling in the other area is with the normal value. Then, the work process of the pacemaker is simulated corresponding to different  $x$ . The relationship of IPT and  $x$  is described in Figure 3.

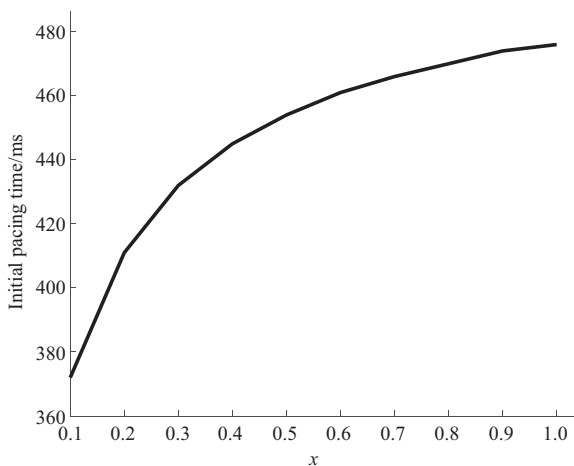


Fig. 3 The relationship between IPT and  $x$

From Figure 3, it is revealed that there is a positive correlation between IPT and  $x$ , which means that IPT becomes longer with the increase of  $x$ . That is, the capacity of pacemaker is weakened by the increasing coupling. What's more, the change rate of IPA increases with the decline of  $x$ , which indicates that the pacemaker is more sensitive to the change of  $x$  when  $x$  becomes smaller.

In addition, we find that the pacemaker paces soundly but it is not able to drive the ventricular tissue when  $x < 0.04$ . The coupling is too weak that the connection between the pacemaker and the ventricle is blocked, leading to the failure of the propagation of the excitation from the pacemaker.

On one hand, the AP of pacemaker is depressed by the surrounding ventricular tissue, and on the other hand, the AP of the tissue is raised by the pacemaker. The electrical connection is controlled by the coupling at the border. If the coupling is too large, the inhibition from the surrounding ventricle becomes

stronger, making the pacemaker a slow pacing or even a failure. On the contrary, if the coupling is too small, the depression to the pacemaker fades, resulting in a wholesome pacing. However, the weak connection leads to a failed propagation of excitation to the ventricular tissue.

After all, the electrical coupling at the border has two sides. The weaker coupling enhances the pacing of the pacemaker and meanwhile restricts the propagation of the excitation to the ventricle.

### 2.3 The APs of cells in special locations

In the section, the effect of the coupling on the APs of the pacing cells and ventricular myocytes is investigated. All the simulation settings are the same as those in Section 2.2.  $x$  is utilized to modulate the coupling at the border. Then the APs of the cells located in special regions are recorded corresponding to different  $x$ . Figure 4 illustrates the APs of the 201<sup>st</sup> cell (the pacing cell at the center of the strand).

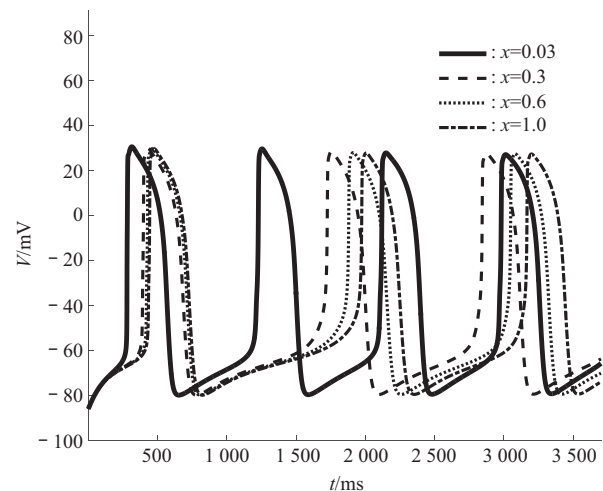


Fig. 4 The APs of the 201<sup>st</sup> cell ( the cell at the center ) corresponding to different  $x$

The solid curve describes the APs for  $x=0.03$ ; the dashed one is the APs for  $x=0.3$ ; the dotted one is the APs for  $x=0.6$  and the dash-dotted one is the APs for  $x=1.0$ , respectively.

According to Figure 4, for different  $x$ , the maximum values of the APs are similar, so are the minimum values. The prominent difference is the periods which enlarge with the promotion of  $x$ . That is, the pacing frequency decreases with the rise of the coupling at the border, which indicates that the capacity of the pacemaker might be weakened by the

larger coupling. The result is consistent with that in Section 2.2.

Figure 5 displays the APs of the 135<sup>th</sup> cell which is the ventricular myocyte located next to the pacemaker corresponding to different  $x$ .

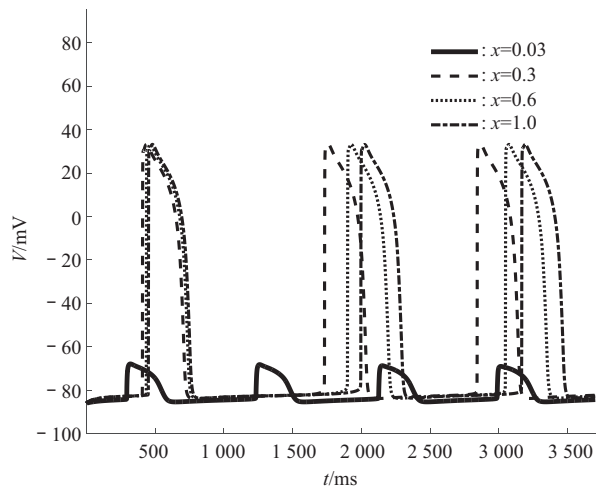


**Fig. 5 The APs of the 135<sup>th</sup> cell ( the ventricular myocyte close to the pacemaker ) corresponding to different  $x$**

The solid curve describes the APs for  $x=0.03$ ; the dashed one is the APs for  $x=0.3$ ; the dotted one is the APs for  $x=0.6$  and the dash-dotted one is the APs for  $x=1.0$ , respectively.

The most prominent feature of Figure 5 is that when  $x=0.03$  the maximum potential value of the myocyte is less than  $-60$  mV, which implies the failure of the depolarization and the block of the propagation. Together with Figure 4, when  $x=0.03$ , the pacemaker paces robustly with a high frequency. However, it is unable to stimulate the adjacent ventricular myocytes to depolarize, leading to the block of the propagation. That is, the weaker coupling results in a strong pacing and meanwhile a fragile driving.

The myocyte depolarizes completely when  $x=0.3, 0.6$  and  $1.0$ . This demonstrates that the excitation from the pacemaker drives the myocyte successfully and propagates through the myocyte to others. From Figure 5, it also suggests that the AP periods of the myocyte change with  $x$ , because the generation of the AP is stimulated by the electrical excitation from the pacemaker, of which the rhythm varies with  $x$ . In addition, the main phases of APs are almost the same for different  $x$ .

#### 2.4 The spatiotemporal propagation

In order to visually observe the propagation of

the electrical excitation in the 1D tissue, both the successful and failed spatiotemporal conductions of the excitation are presented.

From the Section 2.2, it is known that the pacemaker could pace and drive the ventricle soundly when  $x \geq 0.04$ . As a consequence,  $x=0.6$  is chosen for simulation, and the simulation results are shown in Figure 6.

In Figure 6a, the horizontal axis is the timeline and the vertical axis represents the locations of the cells. The column corresponding to any  $t_0$  in horizontal axis depicts the potential distribution of the 1<sup>st</sup> to 401<sup>st</sup> cells at that time, while the row corresponding to any  $n_0$  in vertical axis exhibits the potential distribution of the  $n_0^{\text{th}}$  cell from 1 ms to 3 700 ms. The potential is described by the color, which is high in red and low in blue. The details are listed in the color bar. From the figure, it is revealed that the excitation emerges from the center (the pacemaker) of the strand and propagates to the two ends.

The APs could be observed clearly in Figure 6b. The red curves are the APs of the pacing cells, while the blue ones are the APs of the ventricular myocytes. It is evidently seen that the pacemaker paces first and drives the myocytes to generate complete APs successively.

When  $0.03=x \leq 0.04$ , from the analysis in Section 2.2, it is concluded that the pacemaker paces healthily. However, the excitation could not spread. The simulation results are shown in Figure 7.

In order to display the details of the propagation more obviously, all the regions with potential above  $-60$  mV are set in red color. As a consequence, the potential changes between  $-80$  mV to  $-60$  mV are more pronounced.

It is in evidence that the pacemaker paces soundly (Figure 7a). However, the peak value of the potentials of the adjacent myocytes is less than  $-60$  mV, leading to a defeated depolarization. The peak potential of the myocytes is too low to drive the neighbors to depolarize, resulting in the block of electrical excitation propagation ultimately.

The details of the APs could be detected more distinctly in Figure 7b. There are 4 well-defined phases in the APs of the pacing cells, while for the myocytes, the curves of the APs are almost like straight lines, with no depolarization or repolarization. The excitation from the pacemaker is demolished vastly by the weaker coupling at the border, which is

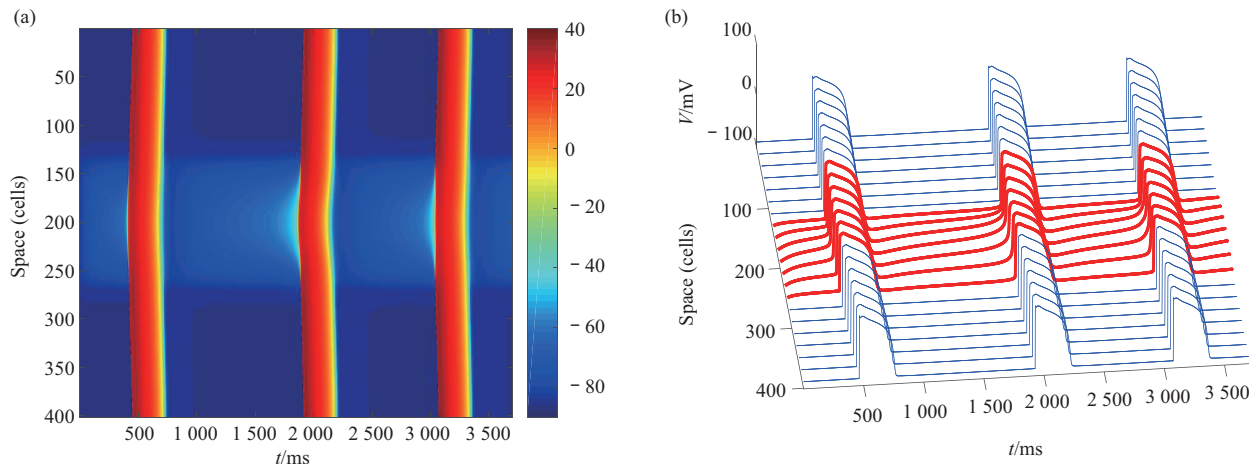


**Fig. 6 Spatial and temporal distribution of the electrical excitation in 1D strand when  $x=0.6$**

(a) The 2D space and time distribution of conductance of the impulses. (b) The 3D space and time distribution of the impulses. The red lines are the APs for pacemaker cells and the blue ones are for working myocytes.

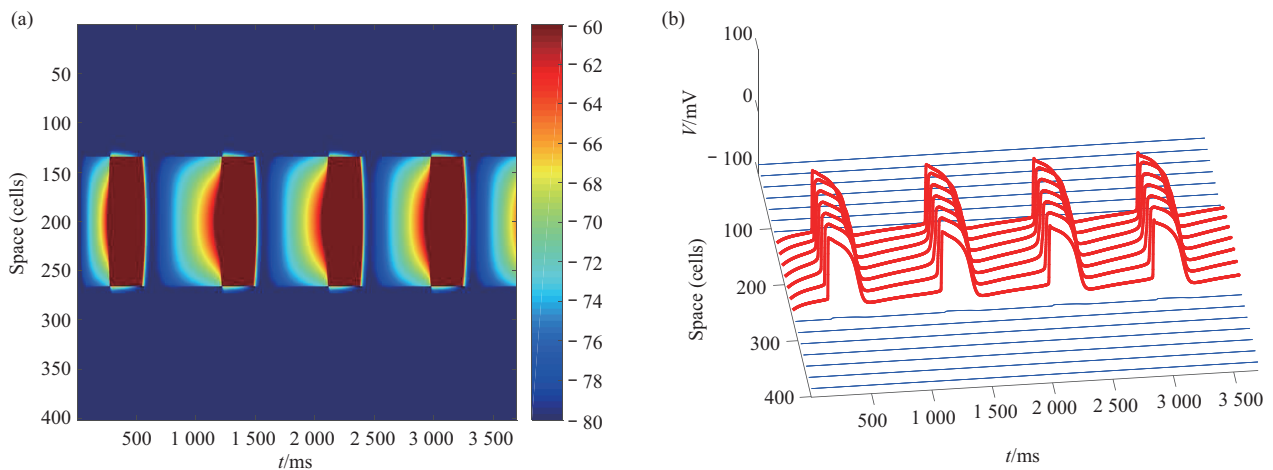


**Fig. 7 Spatial and temporal distribution of the electrical excitation in the 1D strand when  $x=0.03$**

(a) The 2D space and time distribution of conductance of the impulses. (b) The 3D space and time distribution of the impulses. The red lines are the APs for pacemaker cells and the blue ones are for working myocytes.

not able to stimulate the ventricular myocytes effectively.

In summary, the pacing and driving of the pacemaker could be enhanced by weakening the coupling at the border. Nevertheless, a too weak coupling would result in a failure of the propagation.

### 2.5 The minimum number of the pacing cells required

In this section, the minimum number of the pacing cells needed to generate a successful pacing and driving is probed corresponding to different  $x$ .

As stated above,  $x$  is employed to modulate the coupling at the border. For a fixed  $x$ , taking 1 as the step, the number of the pacing cells is increased from 1 until the pacemaker is able to pace and drive the ventricular tissue. And then the corresponding number is recorded, which is the minimum number of the pacing cells required for the  $x$ . The relationship between the number and  $x$  is depicted in Figure 8.

Figure 8 demonstrates that more pacing cells are required to make a successful pacing and driving with the increase of the  $x$ . Nevertheless, the changes are

not significant when  $x > 0.3$ . Taking  $x=1.0$  and  $x=0.25$  for example, the minimum number is 64 for  $x=1.0$ , while it is 61 for  $x=0.25$ . The ratio of the latter to the former is about 95.3%. The pacing cells required are reduced by 4.7%. As a comparison, if the coupling in the whole pacemaker is modulated, the minimum number is 42 981 for  $x=1.0$ , while it is 11 289 for  $x=0.25$ . The ratio is 26.2%<sup>[23]</sup>. The pacing cells required are diminished by 73.8%. This indicates that weakening the coupling alone at the border plays a certain role in the functioning of the biological pacemaker. However, the effect is not prominent.

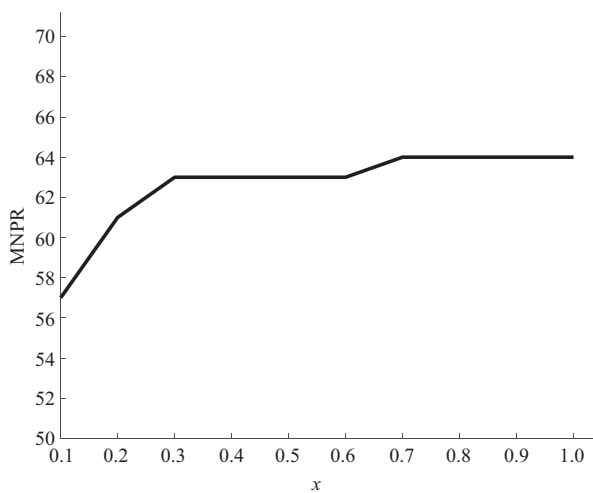


**Fig. 8** The minimum number of pacing cells required ( MNPR ) to make a successful pacing and driving corresponding to different  $x$

## 4 Conclusions

Biological pacemaker has been a hotspot in recent years. However, there are still many key technologies to probe how to create a feasible and effective biological pacemaker.

In the manuscript, the effect of the electrical coupling at the border on the functioning of the biological pacemaker is investigated. Firstly, a 1D computing model containing a biological pacemaker and the ventricular tissue is developed. Based on the model, the IPT, APs in special locations, and the propagation of the excitation are simulated, and it is discovered that the functioning of the pacemaker is promoted with the decline of the coupling at the border. Nevertheless, if the coupling is too weak, the propagation is blocked at the border, though the

pacemaker paces soundly. That is in that the excitation accessing to the ventricular tissue is attenuated extremely by the weaker coupling at the border, not able to stimulate the myocytes to generate complete depolarization.

In addition, from the relationship between the minimum number of the pacing cells required and the electrical coupling at the border, it is found that the former is not influenced manifestly by the latter.

In conclusion, on one hand, the weak electrical coupling at the border plays a positive role in the biological pacemaker, guaranteeing the pacing. On the other hand, the propagation might be blocked by a too weak coupling, leading to an unsuccessful driving. As a consequence, to create an effective and efficient biological pacemaker, it is unfavorable to weaken the coupling at the border alone, and other affecting factors should also be taken into consideration. Moreover, the further investigation on the 2D level will be performed in the following study.

## References

- [1] Zhang J, Zhang B, Wang D, *et al.* Principal component analysis-based heart sound features reduction research. *Journal of Image and Signal Processing*, 2018, 7(4): 213-219
- [2] Greenspon A J, Patel J D, Lau E, *et al.* Trends in permanent pacemaker implantation in the United States from 1993 to 2009 increasing complexity of patients and procedures. *J Am Coll Cardiol*, 2012, 60(16): 1540-1545
- [3] Madhavan M, Mulpuru S K, Mcleod C J, *et al.* Advances and future directions in cardiac pacemakers: Part 2 of a 2-Part Series. *J Am Coll Cardiol*, 2017, 69(2): 211-235
- [4] Bernstein A D, Parsonnet V. Survey of cardiac pacing and implanted defibrillator practice patterns in the United States in 1997. *Pace*, 2001, 24(5): 842-855
- [5] Cingolani E. Biological pacemakers: ready for the clinic?. *Trends Cardiovas Med*, 2015, 25(8): 674-675
- [6] Rosen M R. Gene therapy and biological pacing. *New Engl J Med*, 2014, 371(12): 1158-1159
- [7] Cingolani E, Goldhaber J I, Marban E. Next-generation pacemakers: from small devices to biological pacemakers. *Nat Rev Cardiol*, 2018, 15(3): 139-150
- [8] Gorabi A M, Hajjighasemi S, Khori V, *et al.* Functional biological pacemaker generation by T-Box18 protein expression *via* stem cell and viral delivery approaches in a murine model of complete heart block. *Pharmacol Res*, 2019, 141: 443-450
- [9] Gorabi A M, Hajjighasemi S, Tafti H A, *et al.* TBX18 transcription factor overexpression in human-induced pluripotent stem cells increases their differentiation into pacemaker-like cells. *J Cell Physiol*, 2019, 234(2): 1534-1546

- [10] Saito Y, Nakamura K, Ito H. Cell-based biological pacemakers: progress and problems. *Acta Med Okayama*, 2018, **72**(1): 1-7
- [11] Bleeker W K, Mackaay A J, Masson-Pevet M, *et al.* Functional and morphological organization of the rabbit sinus node. *Circ Res*, 1980, **46**(1): 11-22
- [12] Zhang Y, Wang K Q, Li Q C, *et al.* Pacemaker created in human ventricle by depressing inward-rectifier K<sup>+</sup> current: a simulation study. *Biomed Res Int*, 2016, **2016**: 3830682
- [13] Oren R V, Clancy C E. Determinants of heterogeneity, excitation and conduction in the sinoatrial node: a model study. *Plos Computational Biology*, 2010, **6**(12): e1001041
- [14] Tellez J O, Dobrzynski H, Greener I D, *et al.* Differential expression of ion channel transcripts in atrial muscle and sinoatrial node in rabbit. *Circ Res*, 2006, **99**(12): 1384-1393
- [15] Wiese C, Grieskamp T, Airik R, *et al.* Formation of the sinus node head and differentiation of sinus node myocardium are independently regulated by Tbx18 and Tbx3. *Circ Res*, 2009, **104**(3): 388-397
- [16] Hoogaars W M H, Engel A, Brons J F, *et al.* Tbx3 controls the sinoatrial node gene program and imposes pacemaker function on the atria. *Gene Dev*, 2007, **21**(9): 1098-1112
- [17] Lin X M, Xu Q, Veenstra R D. Functional formation of heterotypic gap junction channels by connexins-40 and-43. *Channels*, 2014, **8**(5): 433-443
- [18] Valiunas V, Weingart R, Brink P R. Formation of heterotypic gap junction channels by connexins 40 and 43. *Circ Res*, 2000, **86**(2): E42-E49
- [19] Valiunas V. Biophysical properties of connexin-45 gap junction hemichannels studied in vertebrate cells. *J Gen Physiol*, 2002, **119**(2): 147-164
- [20] Moreno A P, Laing J G, Beyer E C, *et al.* Properties of gap junction channels formed of connexin 45 endogenously expressed in human hepatoma (SKHep1) cells. *The American Journal of Physiology*, 1995, **268**(2 Pt 1): C356-C365
- [21] Coppen S R, Kodama I, Boyett M R, *et al.* Connexin45, a major connexin of the rabbit sinoatrial node, is co-expressed with connexin43 in a restricted zone at the nodal-crista terminalis border. *The Journal of Histochemistry and Cytochemistry*, 1999, **47**(7): 907-918
- [22] Kreuzberg M M, Sohl G, Kim J S, *et al.* Functional properties of mouse connexin30.2 expressed in the conduction system of the heart. *Circ Res*, 2005, **96**(11): 1169-1177
- [23] Boyett M R, Inada S, Yoo S, *et al.* Connexins in the sinoatrial and atrioventricular nodes. *Adv Cardiol*, 2006, **42**: 175-197
- [24] Kapoor N, Galang G, Marban E, *et al.* Transcriptional suppression of connexin43 by TBX18 undermines cell-cell electrical coupling in postnatal cardiomyocytes. *J Biol Chem*, 2011, **286**(16): 14073-14079
- [25] Kapoor N, Liang W B, Marban E, *et al.* Direct conversion of quiescent cardiomyocytes to pacemaker cells by expression of Tbx18. *Nat Biotechnol*, 2013, **31**(1): 54-62
- [26] Hu Y F, Dawkins J F, Cho H C, *et al.* Biological pacemaker created by minimally invasive somatic reprogramming in pigs with complete heart block. *Sci Transl Med*, 2014, **6**(245): 245ra94
- [27] Zhang Y, Wang K Q, Yang F, *et al.* A simulation study of the bio-pacemaker induced from ventricular myocytes. *Prog Biochem Biophys*, 2016, **43**(12): 1189-1196
- [28] Xie Y F, Sato D, Garfinkel A, *et al.* So Little source, so much sink: requirements for afterdepolarizations to propagate in tissue. *Biophys J*, 2010, **99**(5): 1408-1415
- [29] Ten Tusscher K H W J, Panfilov A V. Alternans and spiral breakup in a human ventricular tissue model. *Am J Physiol-Heart C*, 2006, **291**(3): H1088-H1100

# 边界处电偶联对1D生物起搏器的作用——一种仿真研究\*

张 越<sup>1,2)</sup> 刘书勇<sup>1)\*\*</sup> 黎 捷<sup>3)</sup> 王宽全<sup>4)</sup>

<sup>1)</sup> 哈尔滨工程大学计算机科学与技术学院, 哈尔滨 150001;

<sup>2)</sup> School of Computer Science and Engineering, University of New South Wales, Sydney, NSW 2052, Australia;

<sup>3)</sup> 燕山大学电子工程学院, 秦皇岛 066004;

<sup>4)</sup> 哈尔滨工业大学计算机科学与技术学院, 哈尔滨 150001)

**摘要** 生物起搏器越来越引起学者们的关注. 本文旨在研究边界处的电偶联对生物起搏器起搏及驱动能力的影响. 首先利用各向异性的反应扩散方程, 建立了包含生物起搏器的1D心室组织模型. 基于该模型, 仿真了不同边界电偶联对应的起搏器初次起搏时间、特殊位置细胞的动作电位、心电的传导过程等参考项, 发现减弱边界处的电偶联对生物起搏器的起搏能力具有一定的增强作用; 然而, 当电偶联足够小时, 起搏器的电兴奋却不能有效地传出, 导致其驱动心室组织失败. 另外, 本文探讨了边界电偶联的大小与起搏器最小尺寸之间的关系, 发现电偶联越小, 起搏器成功起搏所需的细胞数量越少, 但是细胞数量变化并不明显. 因此, 仅仅减弱电偶联对生物起搏器有一定的增强作用, 但如果生成高效的起搏器, 仍需辅助其他措施.

**关键词** 生物起搏器, 心室肌细胞, 起搏能力, 驱动能力, 电偶联

**中图分类号** TP391.9, R318.04

**DOI:** 10.16476/j.pibb.2019.0327

---

\* 国家自然科学基金(61701135), 中国博士后科学基金(2018M630342), 黑龙江省自然科学基金(QC2018075)和河北省自然科学基金(F2019203569)资助项目.

\*\* 通讯联系人.

Tel: 13091439889, E-mail: liushuyong@hrbeu.edu.cn

收稿日期: 2019-12-22, 接受日期: 2020-04-03